Phys. Lett. B 861 (2025) 139253

Contents lists available at ScienceDirect

Physics Letters B

journal homepage: www.elsevier.com/locate/physletb

Letter

Disentangling single-particle and collective signatures in ^{12}C(p,2p)^{11}B reaction

E. Cravo [a,b], R. Crespo [c,d,e,*], A. Deltuva [f], D. Jurčiukonis [f]

[a] Departamento de Física, Faculdade de Ciências, Universidade de Lisboa, Campo Grande, 1749-016 Lisboa, Portugal
[b] Centro de Física Teórica e Computacional, Faculdade de Ciências, Universidade de Lisboa, Campo Grande, 1749-016 Lisboa, Portugal
[c] Departamento de Física, Instituto Superior Técnico, Universidade de Lisboa, Av. Rovisco Pais 1, 1049-001, Lisboa, Portugal
[d] Centro de Ciências e Tecnologias Nucleares, Universidade de Lisboa, Estrada Nacional 10, 2695-066 Bobadela, Portugal
[e] Centro de Física e Engenharia de Materiais Avançados, Universidade de Lisboa, Av. Rovisco Pais 1, 1049-001, Lisboa, Portugal
[f] Institute of Theoretical Physics and Astronomy, Vilnius University, Saulėtekio al. 3, LT-10257 Vilnius, Lithuania

ARTICLE INFO

Editor: B. Balantekin

Keywords:
Few-body reactions
Proton removal reactions
Single particle excitations
Collective excitations

ABSTRACT

We calculate kinematically fully exclusive cross sections for the ^{12}C(p,2p)^{11}B reaction at $E_p = 98.7$ MeV proton beam energy, leading to the low-lying states of ^{11}B. We use rigorous three-particle scattering framework extended to include simultaneously and consistently both core excitation and single-particle-like excitations. This predicts significant cross sections for the transitions to the final $\frac{5}{2}^-$ (4.45 MeV) and $\frac{7}{2}^-$ (6.74 MeV) excited states that cannot be populated through the direct single-particle excitation mechanism. We show that these two types of excitations manifest themselves with distinct and characteristic features in the scattering observables.

1. Introduction

Atomic nuclei are bound many-body systems of protons and neutrons interacting by a strong short-range force and Coulomb. To a first approximation many of them can be described by an Independent Particle Model (IPM). In this framework, uncorrelated nucleons move in an average (mean field) potential generated by other nucleons. Since this mean field has central and spin-orbit terms, the energy eigenvalues of the Hamiltonian become distributed in shells. In the nucleus ground state, protons and neutrons fill independently and progressively these shells while satisfying the Pauli exclusion principle. The low-lying spectra is then described by single-particle excitations associated with the promotion of individual nucleons across the shells. The IPM model predicts the well known magic numbers of neutrons and protons, associated with strongly bound nuclei. Furthermore, it is connected with many nuclear properties, including the abundance of the elements. The model is found to be well suited for nuclei with one nucleon extra to a closed shell (core) of nucleons.

On the other hand, due to nucleon correlations, collective aspects associated with vibrational or rotational motion represent an essencial aspect of the nuclear many-body system. The former is associated with a collective oscillation about a spherical shape while the later can only be present when there is permanent nuclear deformation as a whole. Ordered types of motion of nucleons have been standardly identified from large quadrupole moments, the occurrence of electric quadrupole gamma transitions with lifetimes about a hundred times shorter than single particle predictions, characteristic spectra and fission reactions [1]. Furthermore, in light nuclei a strong nuclear deformation can be related to cluster formation appearing in excited states near the corresponding cluster decay energy [2,3].

The collective and cluster formation constitute an essential aspect of both microscopic and large scale structure systems, which determine their evolution. Moreover, the understanding of the coexistence of different aspects of the nuclear many-body system due to nucleon correlations, and its excitation during a scattering process, is a timely issue. Additionally, it is a key milestone for the understanding of nucleon correlations.

Nevertheless, nuclear physics relies on the artificial separation between the Structure and Reaction fields of research. For instance, the single-particle mode aspect has been extracted from one-nucleon knock-out reactions at intermediate and high energies. In these reactions one nucleon is removed from the parent nucleus, ^{A}P, leading to the daughter or residue, $^{A-1}$R, in the ground or any excited state, often without the identification of the final states [4–16]. The standard modelling of

* Corresponding author.
E-mail address: raquel.crespo@tecnico.ulisboa.pt (R. Crespo).

https://doi.org/10.1016/j.physletb.2025.139253
Received 26 November 2024; Accepted 8 January 2025

Available online 10 January 2025

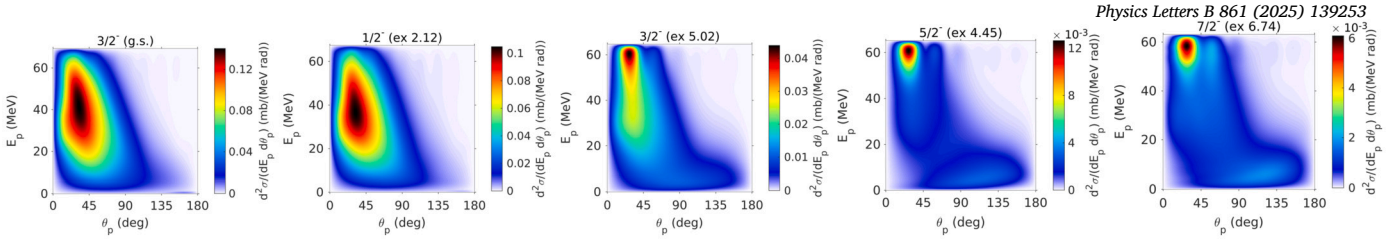

Fig. 1. Contour plot of the energy-angle correlation cross section $\frac{d^2\sigma}{dE_p d\theta_p}$ (units of mb/(MeV rad)) for a measured proton in the center-of-mass (c.m.) frame.

these knockout reactions makes use of a crucial assumption, in which the probe knocks a single nucleon without large momentum transfer to the residue nucleus which participates as a spectator during the reaction process. This way the one-nucleon spectroscopic overlap (SO) and its strength, the so called spectroscopic factor (SF) become the key structure information to be merged in the reaction mechanism [13,17].

Recently, both single-particle and collective excitations (called also core excitations, CX) during the scattering process have been incorporated in few-cluster (core+nucleon+nucleon) nuclear reactions with light nuclei [18–25]. It was found in those works that the dynamical excitation of the nuclear core plays an important role in three-body breakup reactions. The work of [23–25] employs generalized three-body transition operators of Alt, Grassberger, and Sandhas (AGS) [26,27] that include simultaneously both core excitation and single-particle-like excitations, making those contributions mutually consistent, the AGS-CX. In this framework these excitations are coupled dynamically via the potential operator. This framework was applied to the study of ^{12}C(p,2p)^{11}B near $E_p = 100$ MeV in direct kinematics [28] where the excitation of the ^{11}B residue proceeds via its interaction with any of the external nucleons. It was found that the dynamical excitation of the core leads to a significant cross section to the $\frac{5}{2}^-$ (4.45 MeV) final excited state that cannot be populated through a single-particle excitation mechanism. In other words, both single-particle and collective modes need to be taken into account.

In this manuscript, we calculate kinematically semi-inclusive differential cross sections for ^{12}C(p,2p)^{11}B reaction at a proton beam energy $E_p = 98.7$ MeV. Most advanced three-body reaction formalism based on Faddeev-type equations including the core excitation [28] is used. We aim to address the question *Can the signature of both contributions, single-particle and collective excitation modes, be disentangled kinematically in reaction observables?*

2. Results

For clarity, we start by outlining the reaction framework. The physical amplitudes for the breakup process are obtained as the on-shell matrix elements of the breakup operator taken between the initial and final channel states [25,28,29]. The initial two-cluster state, where the proton, p, with a given relative momentum impinges on the composite parent nucleus, ^{A}P, (bound state of the residue nucleus, $^{A-1}$R, and a nucleon, N) has coupled ground- and excited-state core components. The weights of those components are related to the respective spectroscopic factors, SFs, but their sum is normalized to unity. The final three-cluster channel can distinguish between the ground and excited states of the residue.

Thy dynamics model is taken over from Ref. [28] where it is described in more detail. In short, the nucleon-residual nucleus potentials that account for the core excitation are constructed in a standard way using the rotational model [30–32]. Therein, the coupling to the internal nuclear degrees of freedom $\hat{\xi}$ of the residue is introduced via the Woods-Saxon potential radius $R = R_0[1 + \beta_2 Y_{20}(\hat{\xi})]$ with β_2 and $\delta_2 = R_0\beta_2$ the quadrupole deformation parameter and length, respectively. We take the optical potential (OP) parametrization developed by Weppner et al. [33] and $\delta_2 \approx 1.5$ fm consistent with the p-^{11}B inelastic data. For the partial wave where the ^{12}C bound state resides the potential is real, its parameters, given in Table A.1 of Ref. [28], were adjusted to reproduce the experimental nucleon separation energy and the corresponding VMC spectroscopic overlap function [34], normalized to unity. As for the two-nucleon potential the results are insensitive to its choice provided it is a realistic high-precision potential [28].

The ^{11}B residue with ground state (g.s.) of spin/parity $\frac{3}{2}^-$ and excited states $\frac{5}{2}^-$ (4.45 MeV) and $\frac{7}{2}^-$ (6.74 MeV) are taken as members of the $K = \frac{3}{2}^-$ rotational band, while the excited states $\frac{1}{2}^-$ (2.12 MeV) and $\frac{3}{2}^-$ (5.02 MeV) as members of the $K = \frac{1}{2}^-$ rotational band. The weights of the ground- and excited-state residue components, are deduced from the SFs taken from [34], that predicts a very small SFs for the excited state members of the $K = \frac{3}{2}^-$ rotational band.

We start by considering a kinematically complete three-particle breakup experiment where two particles, say α and β are detected. From energy and momentum conservation, the final-state kinematics can be determined completely by their solid angles, Ω_α and Ω_β respectively, and the energy of one of the particles, for example E_α. The corresponding fivefold differential cross section, $\frac{d^5\sigma}{dE_\alpha d\Omega_\alpha d\Omega_\beta}$, is calculated from the amplitude for the three-cluster breakup reaction with the core nucleus in a given final state [28].

From integration of the fully exclusive fivefold differential cross section one readily obtains the semi-inclusive cross sections [11]. For example, the energy-polar angle, $\frac{d^2\sigma}{dE_p d\theta_p}$, the polar-polar angle, $\frac{d^2\sigma}{d\theta_{p_1} d\theta_{p_2}}$, and the polar-azimuthal angle, $\frac{d^2\sigma}{d\theta_p\, d(\Delta\phi)}$ cross sections, where $\Delta\phi$ is the difference in azimuthal angles of the two protons. Note that protons are indistinguishable particles and the scattering amplitudes are correspondingly antisymmetrized [28].

In Fig. 1 we present the calculated contour plot of the energy-polar angle correlation cross sections $\frac{d^2\sigma}{dE_p d\theta_p}$ for a measured proton in the center-of-mass (c.m.) frame. At the zenith of the cross section for the lowest core states in each band, the proton energy is about $E_p \sim 40$ MeV, about half of the energy beam. This is in agreement with what it is expected from a quasi free scattering (QFS) mechanism dominated by the interaction of the proton beam with a target nucleon. As for the transitions to the excited states, we find that proton energy is about $E_p \sim 60$ MeV, near the maximal allowed energy, which means that only a relatively small fraction of the beam proton energy is transferred to other particles, which is a typical case when interacting predominantly with a heavier particle, the core. Thus, while the proton-proton interaction is decisive for the g.s. and $\frac{1}{2}^-$ channels, the proton-core interaction with excitation is decisive for transitions to $\frac{5}{2}^-$ and $\frac{7}{2}^-$ channels, that due to the smallness of their SFs can not be populated via the single-particle excitation mechanism. The $\frac{3}{2}^-$ (5.02 MeV) state with SF around 0.2 is intermediate between the two extreme cases. In $\frac{5}{2}^-$ and $\frac{7}{2}^-$ note also a local maximum at low proton energy and large angle. It corresponds to the proton from the target that did not acquire significant energy and momentum transfer from the beam, as it was absorbed by the core.

In Fig. 2 we show the contour plots of the polar-polar angle correlations for the two measured protons in the c.m. frame. For the transitions to the band heads, the $\frac{3}{2}^-$ (g.s.) and $\frac{1}{2}^-$ (2.12 MeV), the protons are predominantly emitted in the forward direction with an opening an-

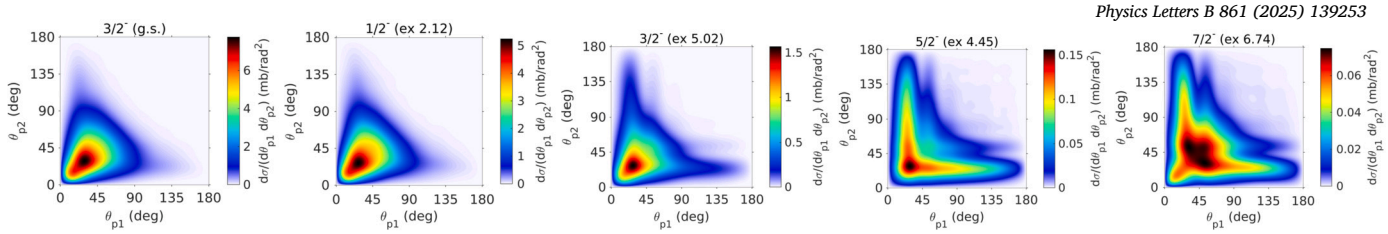

Fig. 2. Contour plot of the angular correlation cross sections $\frac{d^2\sigma}{d\theta_p d\theta_N}$ (in units of mb/rad^2) for measured protons in the c.m. frame.

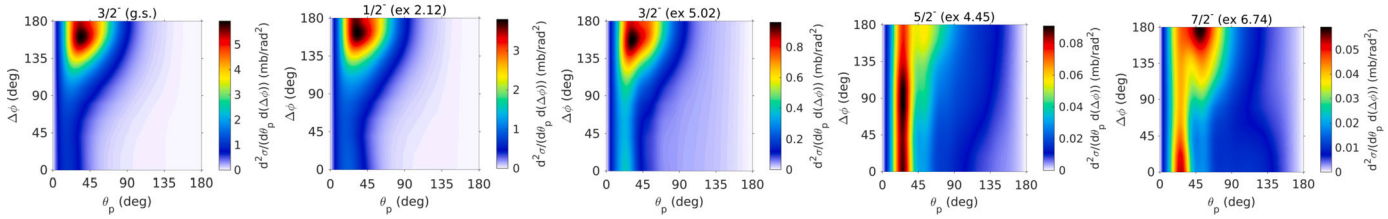

Fig. 3. Contour plot of the polar-azimuthal angle correlations $\frac{d^2\sigma}{d\phi d\theta_N}$ (in units of mb/sr).

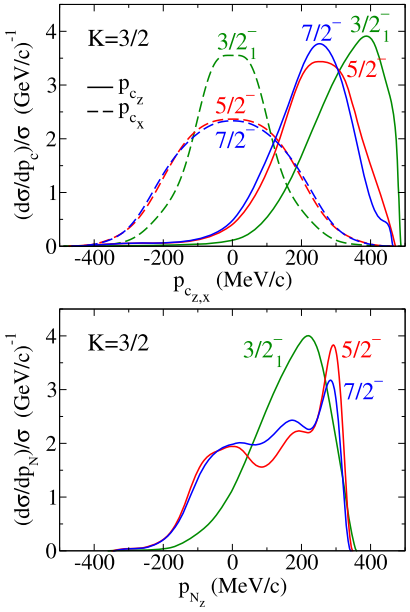

Fig. 4. Calculated heavy fragment (top) and nucleon (bottom) transverse and longitudinal momentum distributions in the c.m. frame, normalized by the total cross section.

gle around the QFS value of 80 degrees [11]. As for the other excited states, and most dominantly in the case of $\frac{5}{2}^-$ and $\frac{7}{2}^-$ transitions, one finds contributions from larger opening angles.

In Fig. 3 we show the contour plots for the polar-azimuthal angle correlations. In the case of the transitions to the band heads, the protons are correlated in coplanar kinematics with a maximum distribution near $\Delta\phi = 180$ degrees. This is consistent with a dominant QFS reaction mechanism. Distinctively, the protons are not correlated in coplanar kinematics for the transitions to the final $\frac{5}{2}^-$ and $\frac{7}{2}^-$ states. For these transitions the polar-azimuthal angle correlation shows comparable contributions from all azimutal angles around the beam axis. Their shape is nevertheless different. The differential cross section is peaked at $\Delta\phi = 90$ degrees for the $\frac{5}{2}^-$ state but has a local minimum at this azimuthal angle for the $\frac{7}{2}^-$ state, respectively. The additional contribution seen at $\Delta\phi = 180$ degrees is similar in both cases.

Moreover, we have found that observables calculated with the Koning and Delaroche (KD) OP parametrization [35] show similar features among the members of the rotational bands although may differ in an overall scale. Therefore, these features of the cross sections appear to be independent of the OP.

Finally, in the top (bottom) part of Fig. 4 we compare the residue (nucleon) transverse and longitudinal momentum distributions (MD) for the $\frac{5}{2}^-$ and $\frac{7}{2}^-$ excited states with those for the ground state. All they are in the c.m. frame and normalized to the respective total cross sections. For excited states the residue transverse MD are considerably wider, and the maxima of the longitudinal MD are located at lower momenta. This indicates a larger momentum transfer to the core in the transitions with core excitation, which is consistent with the proton-core interaction dominance for these transitions.

The nucleon longitudinal MD are strikingly different for the g.s. and $\frac{5}{2}^-$ or $\frac{7}{2}^-$ excited states. In the latter cases one observes a local maximum near zero momentum, that corresponds to the proton from the target emitted with low energy.

3. Difference between transitions to $\frac{5}{2}^-$ and $\frac{7}{2}^-$ states

Next, we get insight on the differences between the polar-azimuthal angle distribution for the transitions to the final residue $\frac{5}{2}^-$ and $\frac{7}{2}^-$ excited states. We present in Fig. 5 the calculations using single-scattering approximation (SSA). As shown in the figure the proton-proton term to the transition amplitude is lower than the proton-core one by two orders of magnitude, due to very small SFs. The dominant proton-core results are quite similar in shape to the full multiple scattering ones given in Fig. 3, but are larger by a factor of 40. Thus, higher-order rescattering effects are extremely important. Nevertheless, qualitative differences between $\frac{5}{2}^-$ and $\frac{7}{2}^-$ azimuthal angle distributions, i.e., maximum vs minimum at $\Delta\phi = 90$ deg, remains also at SSA. This suggests the $\frac{5}{2}^-$ vs $\frac{7}{2}^-$ difference in the polar-azimuthal angle distribution to arise from the proton-core inelastic contributions. This may appear to be quite unexpected, since the p+ ^{11}B inelastic cross sections for $\frac{5}{2}^-$ and $\frac{7}{2}^-$ states due to the quadrupole excitation are of similar shape.

In Fig. 6 we compare the calculated p+ ^{11}B inelastic cross section leading to the $\frac{5}{2}^-$ and $\frac{7}{2}^-$ excited states, and indeed unpolarized cross sections have similar shape. However, when decomposing into contributions with fixed initial spin projections of the ^{11}B g.s., one observes that their behavior differs significantly. For example, the cross section for the $\frac{5}{2}^-$ state with initial spin projection $m_i = \frac{1}{2}$ is larger than with $m_i = \frac{3}{2}$, in opposite to the case of the transition to the $\frac{7}{2}^-$ final state. While in unpolarized two-body scattering those contributions with different ^{11}B initial spin projections simply add together, for three-body ^{12}C(p,2p)^{11}B

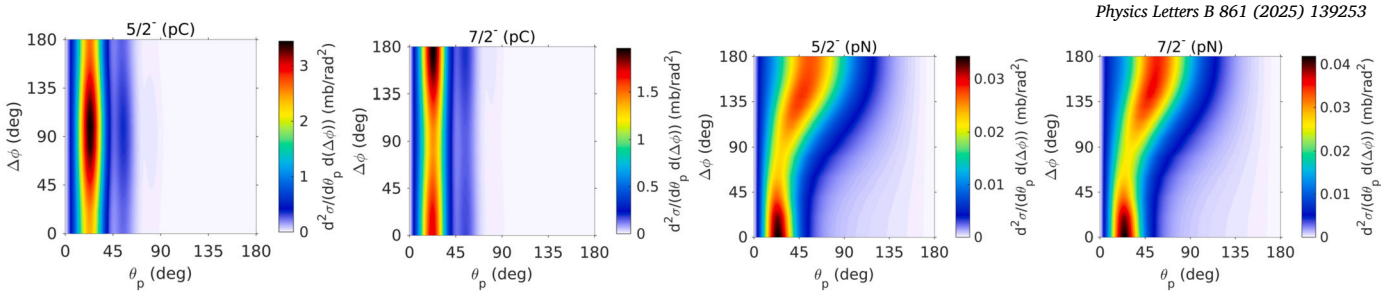

Fig. 5. Contour plot of the polar-azimuthal angle correlations in the SSA considering the proton-core or the proton-proton term only to the transition amplitude.

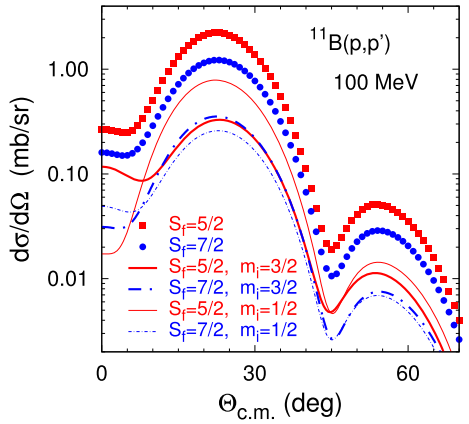

Fig. 6. Differential cross sections for p+ ^{11}B inelastic scattering at 100 MeV leading to the $\frac{5}{2}^-$ (4.45 MeV) and $\frac{7}{2}^-$ (6.74 MeV) excited states. Results with fixed ^{11}B initial spin projections (given by curves) are compared with the total spin-averaged sums (symbols).

SSA amplitude they are weighted by the respective components of the ^{12}C bound state wave function, such that the total angular momentum of ^{12}C, being the sum of ^{11}B spin and nucleon angular momentum, adds to zero. The nucleon part of it carries the angular dependence given by the spherical harmonics, and obviously depends also on the angular momentum projection, giving different weights to $m_i = \frac{1}{2}$ and $m_i = \frac{3}{2}$ components of ^{11}B.

4. Summary and conclusions

We have studied the ^{12}C(p,2p)^{11}B reaction at $E_p = 98.7$ MeV proton beam energy. The ^{11}B ground state with spin/parity $\frac{3}{2}^-$ and excited states $\frac{5}{2}^-$ (4.45 MeV) and $\frac{7}{2}^-$ (6.74 MeV) were taken as members of the $K = \frac{3}{2}^-$ rotational band, while the excited states $\frac{1}{2}^-$ (2.12 MeV) and $\frac{3}{2}^-$ (5.02 MeV) were taken as members of the $K = \frac{1}{2}^-$ rotational band. We used a rigorous three-particle scattering framework that employs generalized three-body transition operators of Alt, Grassberger, and Sandhas extended to include simultaneously and consistently both core- and single-particle-like excitations. This framework predicts a significant cross sections to the low-lying $\frac{5}{2}^-$ (4.45 MeV) and $\frac{7}{2}^-$ (6.74 MeV)] excited states of ^{11}B, associated with very small spectroscopic factors, that cannot be populated through a direct single-particle excitation mechanism.

We show that these two types of excitations manifest themselves with distinct and characteristic features in the scattering observables. The calculated residue transverse momentum distributions for transitions to the $\frac{5}{2}^-$ and $\frac{7}{2}^-$ excited states are considerably wider than to the ground state, and the maxima of the longitudinal MD are located at lower momenta. This is explained by the proton-core interaction dominance in these transitions with the core excitation, that implies a larger momentum transfer to the core as compared to the standard single-particle excitation mechanism. In the proton longitudinal MD for transitions to the $\frac{5}{2}^-$ and $\frac{7}{2}^-$ excited states one identifies a local maximum near zero momentum, that corresponds to the proton from the target emitted with low energy.

Additionally, we have calculated semi-inclusive differential cross sections. For transitions to $\frac{5}{2}^-$ and $\frac{7}{2}^-$ states we find that the protons are not correlated in coplanar kinematics, a signature clearly identified in the polar-azimuthal angle distributions. Moreover, the initial-state spin coupling leads to differences in angular distributions for transitions to $\frac{5}{2}^-$ and $\frac{7}{2}^-$ states.

More experimental data is desirable to further study the signatures of collective excitations.

Declaration of competing interest

The authors declare that they have no known competing financial interests or personal relationships that could have appeared to influence the work reported in this paper.

Acknowledgements

A.D. and D.J. are supported by the Research Council of Lithuania (LMTLT) under Contract No. S-MIP-22-72. Part of the computations were performed using the infrastructure of the Lithuanian Particle Physics Consortium.

Data availability

Data will be made available on request.

References

[1] A. Bohr, B.R. Mottelson, Collective and Invididual aspects of nuclear structure, 1957.
[2] W. Von Oertzen, M. Free, Y. Kanada-Enýo, Phys. Rep. 432 (2006) 43.
[3] Y. Kanada-Enýo, T. Suhara, F. Kobayashi, Eur. Phys. J. 66 (2014) 01008.
[4] V. Panin, et al., Phys. Lett. B 753 (2016) 204.
[5] L. Atar, et al., Phys. Rev. Lett. 120 (2018) 052501.
[6] P. Díaz Fernández, et al., Phys. Rev. C 97 (2018) 024311.
[7] S. Kawase, et al., Prog. Theor. Exp. Phys. 2018 (2018) 021D01.
[8] M. Gómez-Ramos, A.M. Moro, Phys. Lett. B 785 (2018) 511.
[9] M. Holl, et al., Phys. Lett. 795 (2019) 682.
[10] N.T. Toan Phuc, K. Yoshida, K. Ogata, Phys. Rev. C 100 (2019) 064604.
[11] R. Crespo, E. Cravo, A. Deltuva, Phys. Rev. C 99 (2019) 054622.
[12] A. Mecca, E. Cravo, A. Deltuva, R. Crespo, A.A. Cowley, A. Arriaga, R.B. Wiringa, T. Noro, Phys. Lett. B 798 (2019) 134989.
[13] R. Crespo, A. Arriaga, R. Wiringa, E. Cravo, A. Deltuva, A. Mecca, Phys. Lett. B 803 (2020) 135355.
[14] C.A. Bertulani, A. Idini, C. Barbieri, Phys. Rev. C 104 (2021) L061602.
[15] T. Aumann, C. Barbieri, D. Bazin, C.A. Bertulani, A. Bonaccorso, W.H. Dickhoff, A. Gade, M. Gómez-Ramos, B.P. Kay, A.M. Moro, T. Nakamura, A. Obertelli, K. Ogata, S. Paschalis, T. Uesaka, Prog. Part. Nucl. Phys. 118 (2021) 103847.
[16] E. Cravo, R.B. Wiringa, R. Crespo, A. Arriaga, A. Deltuva, M. Piarulli, Phys. Lett. B 859 (2024) 139087.
[17] I. Brida, Steven C. Pieper, R.B. Wiringa, Phys. Rev. C 84 (2011) 024319.
[18] A.M. Moro, R. Crespo, Phys. Rev. C 85 (2012) 054613.
[19] A. Moro, J.A. Lay, Phys. Rev. Lett. 109 (2012) 232502.
[20] N.C. Summers, F.M. Nunes, Phys. Rev. C 76 (2007) 014611.
[21] R. de Diego, J.M. Arias, J.A. Lay, A.M. Moro, Phys. Rev. C 89 (2014) 064609.

[22] R. de Diego, R. Crespo, A.M. Moro, Phys. Rev. C 95 (2017) 044611.
[23] A. Deltuva, Phys. Rev. C 88 (2013) 011601(R).
[24] A. Deltuva, D. Jurčiukonis, E. Norvaišas, Phys. Lett. B 769 (2017) 202.
[25] A. Deltuva, Phys. Rev. C 99 (2019) 024613.
[26] L.D. Faddeev, Zh. Eksp. Teor. Fiz. 39 (1960) 1459, Sov. Phys. JETP 12 (1961) 1014.
[27] E.O. Alt, P. Grassberger, W. Sandhas, Nucl. Phys. B 2 (1967) 167.
[28] A. Deltuva, E. Cravo, R. Crespo, D. Jurčiukonis, Phys. Lett. B 855 (2024) 138859.
[29] R. Crespo, A. Deltuva, M. Rodríguez-Gallardo, E. Cravo, A.C. Fonseca, Phys. Rev. C 79 (2009) 014609.
[30] A. Bohr, B.R. Motelson, Nuclear Structure, World Scientific, Singapore, 1998.
[31] T. Tamura, Rev. Mod. Phys. 37 (1965) 679.
[32] I.J. Thompson, Comput. Phys. Rep. 7 (1988) 167.
[33] S.P. Weppner, R.B. Penney, G.W. Diffendale, G. Vittorini, Phys. Rev. C 80 (2009) 034608.
[34] R.B. Wiringa, https://www.phy.anl.gov/theory/research/overlaps/.
[35] A.J. Koning, J.P. Delaroche, Nucl. Phys. A 713 (2003) 231.